Vacuum 175 (2020) 109257

Contents lists available at ScienceDirect

Vacuum

journal homepage: http://www.elsevier.com/locate/vacuum

Short communication

# Insight into the thermal decomposition properties of potassium perchlorate ($KClO_4$)-based molecular perovskite

Qi Jia [a], Peng Deng [a,b,*], Xiaoxia Li [a], Lishuang Hu [a], Xiong Cao [a,**]

[a] School of Environment and Safety Engineering, North University of China, Taiyuan, 030051, China

[b] State Key Laboratory of Explosion Science and Technology, Beijing Institute of Technology, Beijing, 100081, China

A R T I C L E I N F O

*Keywords:*
Molecular perovskite
($H_2$dabco)[K($ClO_4$)$_3$]
Decomposition property
Thermal analysis
Synergistic catalysis

A B S T R A C T

Studying thermal decomposition properties of the perchlorate-based molecular perovskite energetic materials is essential to facilitate the potential applications. In this work, thermal decomposition properties of potassium perchlorate (KClO4)-based molecular perovskite were investigated. Potassium perchlorate -based molecular perovskite ($H_2$dabco)[K($ClO_4$)$_3$] were prepared by the one-pot reaction of $KClO_4$, $HClO_4$ and triethylenediamine (dabco). The samples were characterized. The results show that ($H_2$dabco)[K($ClO_4$)$_3$] has ternary organic-inorganic perovskite crystal structures. The thermal decomposition results demonstrated that molecular perovskite ($H_2$dabco)[K($ClO_4$)$_3$] has a lower decomposition temperature (383.6 °C) and a higher heat release (2815 J $g^{-1}$) than 607.7 °C and 313 J $g^{-1}$ of the monocomponent $KClO_4$, respectively. The activation energy of thermal decomposition of ($H_2$dabco)[K($ClO_4$)$_3$] had been reduced appreciably from 191.2 kJ $mol^{-1}$ to 177.7 kJ $mol^{-1}$. A synergistic catalysis thermal decomposition mechanism based on unique molecular perovskite structure was proposed. This work offers a novel understanding for thermal decomposition of the molecular perovskite energetic materials.

## 1. Introduction

Molecular perovskite with ternary $ABX_3$-type crystal structures has attracted much attention due to its unique physical, chemical and electronic characteristics, which endow perovskite materials with potential applications, such as energy, catalysis and so on [1–3].

In the field of energetic materials, high-energy-density molecular perovskite energetic materials were pioneered by Chen's group [4.5]. By molecular assembly strategy, high-energy inorganic oxidizer $KClO_4$ and organic fuel dabco were assembled in a crystal cell to form high-symmetry ternary $KClO_4$-based molecular perovskite. Molecular perovskite ($H_2$dabco)[K($ClO_4$)$_3$] with excellent detonation performance and low cost has stronger advantages in future applications [4–10].

However, current research studies concentrate on the design and preparation of $KClO_4$-based energetic composites, mainly including the physical mixed composites in micro/nano scale prepared by the nano metal and its oxides introduced [11–14]. $KClO_4$ with inherent properties (i. e. the higher thermal decomposition temperature, the higher activation energy, and the low heat release) hinders its potential applications in a deeper level [15,16], although people always have a desire to improve the thermal decomposition performance and energy-releasing efficiency of $KClO_4$.

Molecular perovskite ($H_2$dabco)[K($ClO_4$)$_3$] with excellent properties undoubtedly provides a new way to promote future applications of $KClO_4$-based energetic materials in modern military and industrial fields [17–20]. But, there is no report for studying thermal decomposition properties of $KClO_4$-based molecular perovskite ($H_2$dabco)[K($ClO_4$)$_3$]. It is therefore important to study the thermal decomposition behavior of $NaClO_4$-based molecular perovskite. It is also essential to understand their thermal decomposition performance and thermodynamics for the future applications [21,22].

Herein, $KClO_4$-based molecular perovskite ($H_2$dabco)[K($ClO_4$)$_3$] was prepared by the one-pot reaction of $KClO_4$, $HClO_4$, and dabco with the molar ratio of 1:2:1. The chemical structure of sample was characterized, and the thermal decomposition behavior and thermodynamics were investigated. Based on the organic-inorganic molecular perovskite structures, a synergistic catalysis thermal decomposition mechanism was proposed.

* Corresponding author. School of Environment and Safety Engineering, North University of China, Taiyuan, 030051, China.
** Corresponding author.
*E-mail addresses:* nash_deng@163.com (P. Deng), cx92rl@163.com (X. Cao).

https://doi.org/10.1016/j.vacuum.2020.109257
Received 4 November 2019; Received in revised form 3 February 2020; Accepted 10 February 2020
Available online 12 February 2020

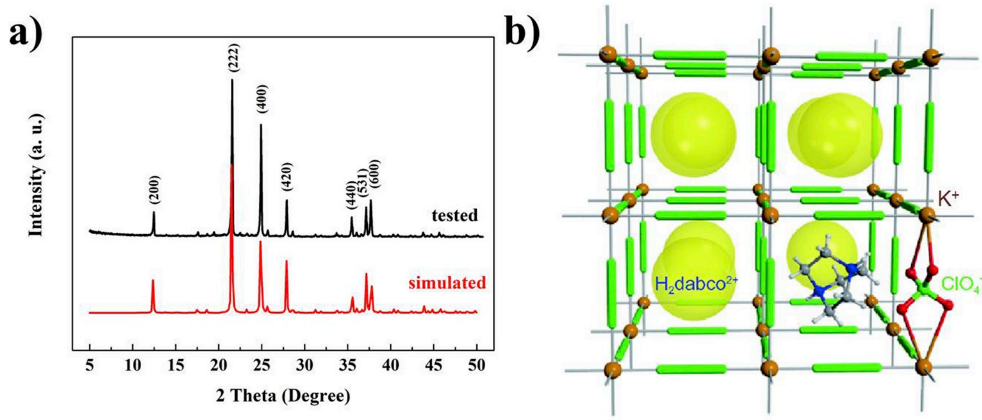


**Fig. 1.** (a) P-XRD patterns and (b) the schematic of perovskite structure of $(H_2dabco)[K(ClO_4)_3]$ [25].

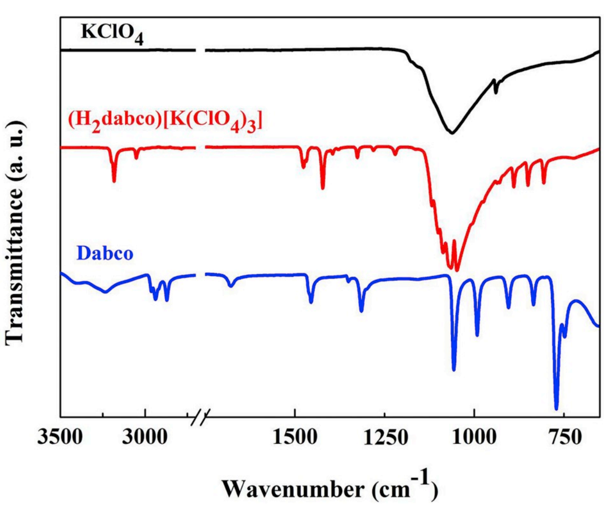


**Fig. 2.** FT-IR spectra of samples: $KClO_4$ (Black), $(H_2dabco)[K(ClO_4)_3]$ (Red), and Dabco (Blue). (For interpretation of the references to colour in this figure legend, the reader is referred to the Web version of this article.)

## 2. Experimental

$KClO_4$ and perchloric acid (70%) were provided from Shanxi Jiangyang Chem. Eng. Co., Ltd. Dabco ($C_6H_{12}N_2$) was provided by Shanghai Aladdin Biochemical Technology Technology Co., Ltd. Deionized water was made in our laboratory. In a typical experimental, 0.138 g $KClO_4$ (0.1 mmol), 0.112 g dabco (0.1 mmol), and 0.163 ml $HClO_4$ (~0.2 mmol) were added successively and dissolved into 20 ml deionized water at 25 °C for 1 h. The mixture was placed in the room. And then crystalline naturally. The samples were obtained by filtration, washing and drying.

Powder X-ray diffraction (P-XRD) patterns were collected on a Philips X'Pert Pro X-ray diffractometer by using Cu-Kα (40 kV, 40 mA) radiation (PANalytical, Holland). Particle sample was milled slightly before tested. Fourier transform infrared (FT-IR) spectrums were recorded on a Nicolet iS 50 spectrophotometer (Thermo Scientific, USA). Pressed KBr pellets were used to test the chemical bonding of the samples from 4000 to 650 $cm^{-1}$. The thermal decomposition process were performed by a STA449F3 thermo-gravimetric/differential scanning calorimeter (TG-DSC, Netzsch, Germany) by a heating rates of 5, 10, 15, and 20 $°C \cdot min^{-1}$. The sample with sample mass: 0.5 mg was tested in an Ar atmosphere over the temperature ranged from 50 to 900 °C. At least three groups of test samples are tested, and the uncertainties in TG-DSC measurements are less than 5%.

## 3. Results and discussions

The P-XRD pattern of as-prepared molecular perovskite $(H_2dabco)[K(ClO_4)_3]$ shows in Fig. 1a. The diffraction peaks at 12.5°, 21.6°, 24.9°, 27.8°, 37.1° and 38.9° corresponded to the crystal planes (200), (222), (400), (420), (531), and (600), respectively, which is in a great agreement with the simulated powder XRD pattern (CCDC:1528106). According to the literatures [23,24], the crystal structure of $(H_2dabco)[K(ClO_4)_3]$ is the perovskite structure $ABX_3$ type, where protonated $H_2dabco^{2+}$ was regarded as the A-site cation, $K^+$ as the B-site cation, and $ClO_4^-$ as the X-bridges.

As shown in Fig. 1b, $K^+$ is located on the corners, face and body centers of the cubic cell, and is interacted by twelve oxygen atoms from six $ClO_4^-$. Meanwhile, $ClO_4^-$ can be considered as bridges with ambient two $K^+$, forming a three-dimensional anionic cage-like framework. Protonated $H_2dabco^{2+}$ is embedded in anionic cages to balance the

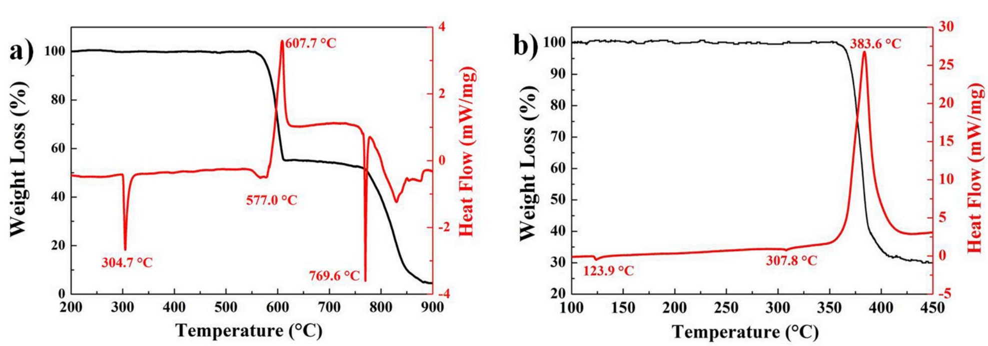


**Fig. 3.** TG -DSC curves of (a) $KClO_4$ and (b) $(H_2dabco)[K(ClO_4)_3]$.

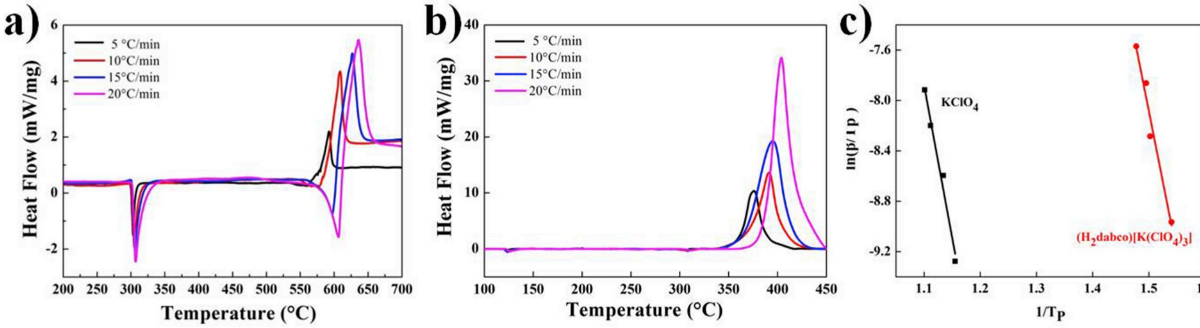


**Fig. 4.** DSC curves of (a) $KClO_4$ and (b) $(H_2dabco)[K(ClO_4)_3]$ at different heating rates, (c) Dependence of $\ln(\beta/T_p^2)$ on $1/T_p$ for samples. Scatter points are experimental data and lines denotes the linear fitting results.

overall charged to zero. The hydrogen bonds were formed by $H_2dabco^{2+}$ and $ClO_4^-$ ligands, resulting in constructing the stable perovskite structure.

The FT-IR spectrums were shown in Fig. 2. The spectrum peaks at 1061 and 939 $cm^{-1}$ are corresponding to $ClO_4^-$ from monocomponent $KClO_4$. And for dabco, the main peaks at 1056, 908, and 835 $cm^{-1}$ are originated from dabco skeletal motion. The attributions of other peaks were also discussed. The peaks at 3235, 2937, 2870, and 991 $cm^{-1}$ correspond to $CH_2$, the peaks at 1678, 1455 $cm^{-1}$ to $CH_2$, and the peak at 1314 $cm^{-1}$ to C–N. For $(H_2dabco)[K(ClO_4)_3]$, the main oxidant group $ClO_4^-$ are located at 1064 $cm^{-1}$ and dabco skeletal motion at 1048, 890, and 850 $cm^{-1}$, which indicated that the main functional groups existed in the molecular perovskite structure. FT-IR spectrum showed C–H vibrational bonds appeared red shift due to the formation of C–H···O hydrogen bonds from $H_2dabco^{2+}$ to $ClO_4^-$.

The thermal properties of the samples were investigated in Fig. 3. For $KClO_4$ in Fig. 3a, the endothermic peaks appeared at 304.7 °C and 577.0 °C, which corresponds to thermotropic phase transitions in the DSC curve. The thermal decomposition of $KClO_4$ occurred at 607.7 °C. But incomplete thermal decomposition can be found at this stage. With the temperature raised, the decomposition product continues to start phase transformation at 769.6 °C and thermal decomposition further at higher temperature. With the formation of molecular perovskite structure of $KClO_4$, $(H_2dabco)[K(ClO_4)_3]$ have only one individual decomposition stage and a lower thermal decomposition temperature 383.6 °C in Fig. 3b. A quick heat release followed immediately with the weight loss of 75%. And the value of heat release is up to 2815 J $g^{-1}$, which is higher than $KClO_4$ (313 J $g^{-1}$). Based on CO for $C_aH_bN_cK_dCl_eO_f$, the oxygen balance was calculated were calculated by: $OB[\%] = 1600[\text{f-a-(b-e} + \text{d)}/2]/M_W$, where $M_W$ of $(H_2dabco)[K(ClO_4)_3]$ is molecular weight [25]. The value of *OB* is 0% here. It demonstrated molecular perovskite $(H_2dabco)[K(ClO_4)_3]$ combined with the oxidizer $ClO_4^-$ and fuel $H_2dabco^{2+}$ can release more heat energy by redox reaction.

The thermal decomposition dynamics of the samples were studied further by DSC with different heating rates. The $KClO_4$ and $(H_2dabco)[K(ClO_4)_3]$ were investigated together in Fig. 4. The kinetic parameters for thermal decomposition were calculated by kissinger Equation (1) [26]:

$$\ln\frac{\beta}{T_p{}^2} = \ln\frac{AR}{Ea} - \frac{Ea}{RT_p} \tag{1}$$

Where $\beta$ is the heating rate in degrees Celsius per minute, $T_p$ is the peak temperature in the DSC curve at that rate. $R$ is the gas constant, $E_a$ is the apparent activation energy and $A$ is the pre-exponential factor.

Fig. 4 shows the DSC curves of $KClO_4$ and $(H_2dabco)[K(ClO_4)_3]$. In Fig. 4c, the reaction activation energy ($E_a$) of main decomposition processes was calculated to be 191.2 kJ $mol^{-1}$. Based on the ternary molecular perovskite structure, the $E_a$ of $(H_2dabco)[K(ClO_4)_3]$ decomposition processes have reduced to 177.7 kJ $mol^{-1}$, which decreased by 13.5 kJ $mol^{-1}$ compared with monocomponent $KClO_4$. That indicated the molecular perovskite $(H_2dabco)[K(ClO_4)_3]$ is easier to be activated under the thermal stimuli.

To study the synergistic catalysis thermal decomposition mechanism of $(H_2dabco)[K(ClO_4)_3]$, coupled thermal analysis techniques TG-QMS were used to perform real-time and continuous analysis of the whole decomposition process. Protonated $H_2dabco^{2+}$ in the ternary molecular perovskite system can be activated and render protons to $ClO_4^-$ with the heating stimuli [19]. But activated protonated $H_2dabco^{2+}$ cannot escape from the three-dimensional anionic cage-like frameworks, because of strong Coulomb forces between $K^+$ and $ClO_4^-$. That resulting in thermal stabilities at lower temperature (<300 °C), as shown in Figs. 3b and 5a. When the heating energy is higher than Coulomb forces, the anionic frameworks will collapse. Accelerated activated protonated $H_2dabco^{2+}$ can facilitates proton transfer easily from $H_2dabco^{2+}$ to $ClO_4^-$ and then the formation of a large number of $HClO_4$, although a few escaped as shown in Fig. 5b, when the anionic frameworks collapsed. With the

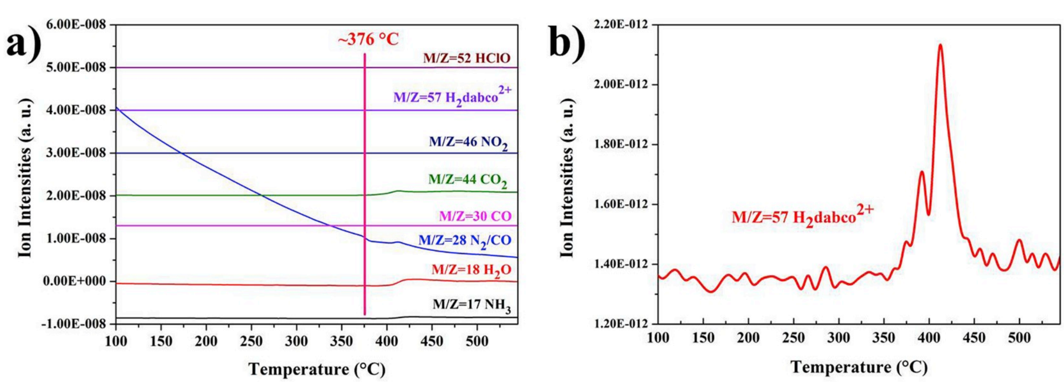


**Fig. 5.** (a) The mass spectra for $(H_2dabco)[K(ClO_4)_3]$ at a heating rate of 20 °C·$min^{-1}$, and (b) The curve of the mass spectra the $m/z$ = 57$H_2dabco^{2+}$ gaseous product.

decomposition of $HClO_4$ sequentially, superoxide radicals ($O_2^-$) were produced and reacted with the fuel dabco. More heat would be released.

Compared with the monocomponent $KClO_4$, The organic molecular fuel dabco was introduced to assemble $KNO_3$-based molecular perovskite. The unique molecular perovskite structures in a cubic cell facilitate the oxidizer and fuel at the molecular scale. More heat release can be obtained by the reaction between the oxidizer and fuel under heating simulated. And the lower thermal decomposition temperature and activated energy also could efficiently support more potential applications in the explosives and propellant fields.

## 4. Conclusions

In summary, thermal decomposition properties of potassium perchlorate (KClO4)-based molecular perovskite were investigated. ($H_2$dabco)[K($ClO_4$)$_3$] with hybrid molecular perovskite structure has a lower decomposition temperature (383.6 °C) than $KClO_4$ (607.7 °C). The high heat release (2815 J $g^{-1}$), which is seven times higher than $KClO_4$ (313 J $g^{-1}$), was obtained from the combination with the oxidizer $KClO_4$ and fuel dabco in the molecular perovskite structure. By thermodynamics analyzed, The activation energy $E_a$ (177.7 kJ $mol^{-1}$) of ($H_2$dabco)[K($ClO_4$)$_3$] was obtained, which is lower than $KClO_4$ (191.2 kJ $mol^{-1}$). The synergistic catalysis thermal decomposition mechanism of ($H_2$dabco)[K($ClO_4$)$_3$] towards improving thermal decomposition and heat energy release was proposed. This work provides a deeper understanding towards further applications of $KClO_4$-based molecular perovskite in advanced explosives and propellants.

## Declaration of competing interest

The authors declare no conflict of interest. The founding sponsors had no role in the design of the study; in the collection, analyses, or interpretation of data; in the writing of the manuscript, and in the decision to publish the results.


## Acknowledgment

This work was supported by Natural Science Foundation of China (21975227). Authors thank Prof. Weixiong Zhang and Dr. Shaoli Chen (Sun Yat-Sen University, Guangzhou, China) for support and help.


## References


[1] T. Liu, Y. Zhou, Q. Hu, Fabrication of compact and stable perovskite films with optimized precursor composition in the fast growing procedure, Sci. China Mater. 60 (2017) 608–616.

[2] J. Ding, Q. Yan, Progress in organic-inorganic hybrid halide perovskite single crystal: growth techniques and applications, Sci. China Mater. 60 (2017) 1063–1078.

[3] H. Bostrom, J. Hill, A. Good, Win Columnar shifts as symmetry-breaking degrees of freedom in molecular perovskites, Phys. Chem. Chem. Phys. 18 (2016) 31881–31894.

[4] P. Deng, Y. Liu, P. Luo, J. Wang, Y. Liu, D. Wang, et al., Two-steps synthesis of sandwich-like graphene oxide/LLM-105 nanoenergetic composites using functionalized graphene, Mater. Lett. 194 (2017) 156–159.

[5] R. Thiruvengadathan, S. Chung, S. Basuray, B. Balasubramanian, C. Staley, K. Gangopadhyay, et al., A versatile self-assembly approach toward high performance nanoenergetic composite using functionalized graphene, Langmuir 30 (2014) 6556–6564.

[6] J. Xu, S. Zheng, S. Huang, Y. Tian, Y. Liu, H. Zhang, et al., Host–guest energetic materials constructed by incorporating oxidizing gas molecules into an organic lattice cavity toward achieving highly-energetic and low-sensitivity performance, Chem. Commun. 55 (2019) 909–912.

[7] P. Deng, J. Xu, S. Li, S. Huang, H. Zhang, J. Wang, et al., A facile one-pot synthesis of monodisperse hollow hexanitrostilbenepiperazine compound microspheres, Mater. Lett. 214 (2018) 45–49.

[8] J. Lei, Q. Guo, D. Yin, X. Cui, R. He, T. Duan, et al., Bioconcentration and bioassembly of N/S co-doped carbon with excellent stability for supercapacitors, Appl. Surf. Sci. 488 (2019) 316–325.

[9] X. Cao, Y. Shang, K. Meng, G. Yue, L. Yang, Y. Liu, et al., Fabrication of three-dimensional TKX-50 network-like nanostructures by liquid nitrogen-assisted spray freeze drying method, J. Energetic Mater. 37 (2019) 356–364.

[10] J. Lei, H. Liu, D. Yin, L. Zhou, J. Liu, Q. Chen, et al., Boosting the loading of metal single atoms via a bioconcentration strategy, Small 16 (2020), 1905920.

[11] A. Ambekar, J. Yoh, A reduced order model for prediction of the burning rates of multicomponent pyrotechnic propellants, Appl. Therm. Eng. 130 (2018) 492–500.

[12] D. Ouyang, G. Pan, H. Guan, C. Zhu, X. Chen, Effect of different additives on the thermal properties and combustion characteristics of pyrotechnic mixtures containing the $KClO_4$/Mg-Al alloy, Thermochim. Acta 513 (2011) 119–123.

[13] M. Cooper, M. Oliver, The burning regimes and conductive burn rates of titanium subhydride potassium perchlorate ($TiH_{1.65}$/$KClO_4$) in hybrid closed bomb-strand burner experiments, Combust. Flame 160 (2013) 2619–2630.

[14] X. Ji, Y. Liu, Z. Li, Q. Yu, Y. Gao, H. Zhang, L. Wang, Thermal behavior of Al/Zr/$KClO_4$ pyrotechnic compositions at high temperature, Thermochim, Acta 659 (2018) 55–58.

[15] M. Rehwoldt, Y. Yong, H. Wang, S. Holdren, M. Zachariah, Ignition of nano-scale titanium/potassium perchlorate pyrotechnic powder: reaction mechanism study, J. Phys. Chem. C 122 (2018) 10792–10800.

[16] Y. Sun, L. Liu, H. Ren, Q. Jiao, The influence of Zr on the decomposition of $KClO_4$, Chin. J. Energetic Mater. 25 (2017) 396–402.

[17] P. Deng, H. Ren, Q. Jiao, Enhanced thermal decomposition performance of sodium perchlorate by molecular assembly strategy, Ionics 26 (2020) 1039–1044.

[18] P. Deng, H. Ren, Q. Jiao, Enhanced the combustion performances of ammonium perchlorate-based energetic molecular perovskite using functionalized graphene, Vacuum 169 (2019), 108882.

[19] J. Zhou, L. Ding, F. Zhao, B. Wang, J. Zhang, Thermal studies of novel molecular perovskite energetic material ($C_6H_{14}N_2$)[$NH_4$($ClO_4$)$_3$], Chin. Chem. Lett. 31 (2020) 554–558.

[20] Q. Jia, X. Bai, S. Zhu, X. Cao, P. Deng, L. Hu, Fabrication and characterization of nano ($H_2$dabco)[K($ClO_4$)$_3$] molecular perovskite by ball milling, J. Energ. Mater (2020), https://doi.org/10.1080/07370652.2019.1698675.

[21] P. Deng, H. Wang, X. Yang, H. Ren, Q. Jiao, Thermal decomposition and combustion performance of high-energy ammonium perchlorate-based molecular perovskite, J. Alloy Compd (2020), https://doi.org/10.1016/j.jallcom.2020.154257.

[22] P. Deng, Q. Jiao, H. Ren, Synthesis of nitrogen-doped porous hollow carbon nanospheres with a high nitrogen content: A sustainable synthetic strategy using energetic precursors, Sci. Total Environ. 714 (2020) 136725.

[23] S. Chen, Z. Yang, B. Wang, Y. Shang, L. Sun, C. He, et al., Molecular perovskite high-energetic materials, Sci. China Mater. 61 (2018) 1123–1128.

[24] Z. Jin, Y. Pan, X. Li, M. Hu, L. Shen, Diazabicyclo[2.2.2]octane-1,4-diium occluded in cubic anionic coordinated framework: the role of trifurcated hydrogen bonds of N–H· · ·O and C–H· · ·O, J. Mol. Struct. 660 (2003) 67–72.

[25] S. Chen, Y. Shang, C. He, L. Sun, Z. Ye, W. Zhang, et al., Optimizing the oxygen balance by changing the A-site cations in molecular perovskite high-energetic materials, CrystEngComm 20 (2018) 7458–7463.

[26] L. Hu, Y. Liu, S. Hu, Y. Wang, 1T/2H multi-phase MoS2 heterostructures: synthesis, characterization and thermal catalysis decomposition of dihydroxylammonium5,5-bistetrazole-1,1-diolate, New J. Chem. 43 (2018) 10434–10441.